Upscaled flow and transport properties for heterogeneous unsaturated media

Raziuddin Khaleel

Fluor Federal Services, Richland, Washington, USA

T.-C. Jim Yeh

Department of Hydrology and Water Resources, University of Arizona, Tucson, Arizona, USA

Zhiming Lu

Earth and Environmental Science Division, Los Alamos National Laboratory, Los Alamos, New Mexico, USA

Received 6 November 2000; revised 5 November 2001; accepted 5 November 2001; published 11 May 2002.

[1] To represent a heterogeneous unsaturated medium by its homogeneous equivalent, stochastic theory-based analytical formulas and numerical Monte Carlo simulations are used to obtain upscaled (effective) flow and transport properties. The Monte Carlo experiments simulate steady state flow and transient transport of nonreactive solute in two-dimensional heterogeneous media. Constitutive relations for unsaturated media at the mesh-size scale are based on the van Genuchten-Mualem relationships. A unit-mean-gradient approach is used to derive upscaled properties for flow parallel and perpendicular to bedding. Upscaled moisture retention and unsaturated conductivities (K) and longitudinal dispersivities are obtained by simulating steady gravity drainage conditions for a series of applied infiltration rates, characteristic of relatively dry conditions in coarse-textured sediments. Macrodispersivities are calculated on the basis of spatial moments of the ensemble-mean plume. Results show that the calculated effective unsaturated K based on the analytical formulas compare well with those based on Monte Carlo simulations. The macroscopic anisotropy (ratio of K parallel to bedding to K perpendicular to bedding) increases with increasing tension, although the increase is rather mild. The longitudinal macrodispersivity for the equivalent homogeneous medium also increases with increasing tension. A comparison of numerical results with stochastic solutions suggests that the computed dispersivities are of the same order of magnitude at low tensions. At higher tensions the dispersivity estimates deviate significantly. Nonetheless, both numerical and analytical results show that the longitudinal dispersivities for flow parallel to bedding are higher than those for flow perpendicular to bedding. In addition, our results suggest that the Fickian regime is reached much earlier for cases with flow perpendicular to bedding than for those with flow parallel to bedding. *INDEX TERMS:* 1869 Hydrology: Stochastic processes; 1875 Hydrology: Unsaturated zone; 1866 Hydrology: Soil moisture; 1829 Hydrology: Groundwater hydrology; *KEYWORDS:* vadose zone, spatial variability, numerical modeling, stochastic processes, effective properties, equivalent media

1. Introduction

[2] Geologic formations are heterogeneous at various length scales. A conventional approach to modeling flow and transport in geological formations is to incorporate into models the overall heterogeneity of the system such as geologic layering. An alternative approach is to define an equivalent homogeneous medium with upscaled (effective or macroscopic) flow and transport properties and thereby predict the mean flow and transport behavior at the field scale [*Yeh*, 1998]. However, to represent a heterogeneous medium by its homogeneous equivalent, one needs to estimate the effective flow and transport properties that represent this equivalent homogeneous medium.

[3] Numerous studies have investigated the effective flow and transport properties for geological formations under saturated conditions [see *Gelhar*, 1993]. Few studies have investigated the effective properties for partially saturated media. Theoretical work [e.g., *Mualem*, 1984; *Yeh et al.*, 1985a, 1985b; *Mantoglou and Gelhar*, 1987; *Green and Freyberg*, 1995], numerical simulations [e.g., *Yeh*, 1989; *Desbarats*, 1998; *Wildenschild and Jensen*, 1999b; *Bagtzoglou et al.*, 1994; *Polmann et al.*, 1991; *Ababou*, 1988] and experimental studies [e.g., *Stephens and Heermann*, 1988; *Yeh and Harvey*, 1990; *McCord et al.*, 1991; *Wildenschild and Jensen*, 1999a] of unsaturated flow indicate that the effective hydraulic conductivity (K) tensor for stratified sediments can exhibit moisture or tension-dependent anisotropy. That is, the anisotropy (ratio of K parallel bedding to K perpendicular to bedding) increases with increasing tension. For solute transport, several studies [e.g., *Mantoglou and Gelhar*, 1985; *Polmann*, 1990; *Russo*, 1993; *Harter and Yeh*, 1996; *Roth and Hammel*, 1996; *Birkholzer and Tsang*, 1997] suggest that the macrodispersivity in unsaturated media increases with a decrease in saturation. While these results are interesting, most of the studies have focused on the flow and transport behavior in coarse-textured media for tension values that are on the order of 100 cm. Furthermore, few studies have investigated the effect of orientation of geological structures (i.e., layering) on the flow and solute transport behavior. The objective of this work is to investigate the effective flow and transport properties for unsaturated coarse-textured media under relatively dry conditions (tensions as high as

0043-1397/02/2000WR000072$09.00

Table 1. Mean and Standard Deviation of Parameters for the van Genuchten-Mualem Model

Parameter	Mean	Standard Deviation
Ln K_s, m/d	0.752	0.627
Ln α, 1/m	1.460	0.341
Ln n	0.600	0.089
θ_s	0.397	0.031
θ_r	0.027	0.004

20 m) that are prevalent in arid regions of the western United States. Also examined is the effect of orientation of bedding on the flow and transport properties; the numerical results are compared with results based on stochastic solutions.

2. Effective Parameters for Flow and Transport

[4] Consider steady infiltration through a vertical heterogeneous unsaturated medium in the $x-z$ plane that is visualized as a collection of many porous elements. Each element has an isotropic hydraulic conductivity, $K(\psi)$, which varies with pressure head, ψ. The steady flux, q, in each element is described by Darcy's law:

$$q = -K(\psi)\nabla(\psi + z). \tag{1}$$

Suppose that the hydraulic conductivity, $K(\psi)$, in the $x-z$ plane, is a stochastic process. Thus there exists an infinite number of realizations of such conductivities and corresponding pressure head fields and fluxes.

[5] An effective conductivity can be viewed as the ability of a fictitious medium to transmit the ensemble mean flux, $\langle q\rangle$, under the ensemble mean hydraulic gradient, $\langle J\rangle$, with $\langle\rangle$ denoting the ensemble average. If the ensemble averages, $\langle q\rangle$ and $\langle J\rangle$, are equivalent to averages over a field-scale representative elementary volume (FSREV), then the effective K of the fictitious medium is referred to as the effective conductivity for an equivalent homogeneous medium [*Yeh*, 1998]. The governing steady state flow equation for the equivalent homogeneous medium then takes the form

$$\nabla\cdot\{K^e(\langle\psi\rangle)\nabla(\langle\psi\rangle + z)\} = 0, \tag{2}$$

where K^e is the unconditional effective unsaturated K, the proportionality constant between $\langle q\rangle$ and $\langle J\rangle$.

[6] Consider solute movement in the same heterogeneous media used to describe the effective flow parameters. Suppose that the solute concentration, C, is a spatial stochastic process as a result of random velocity due to random gradient and conductivity field. The ensemble mean convection-dispersion equation for the unsaturated zone is [*Mantoglou and Gelhar*, 1985; *Harter and Yeh*, 1996]

$$\nabla\cdot\left(D_{ij}\nabla\langle C\rangle\right) - \langle V\rangle\cdot\nabla\langle C\rangle = \frac{\partial\langle C\rangle}{\partial t}, \tag{3}$$

where $\langle V\rangle$ is the mean velocity and is equal to $\langle q\rangle/\langle\theta\rangle$; $\langle\theta\rangle$ is the mean moisture content and D_{ij} is the macrodispersion coefficient tensor, which represents dispersion caused by variations in velocity at scales smaller than the FSREV. If we assume that the macrodispersion coefficient is linearly proportional to the mean velocity, the constant of proportionality is called the macrodispersivity. Note that the ensemble mean equations (2) and (3) have the same form as those of the laboratory-scale problem, implying that the laboratory-scale equations can be scaled up for field-scale problems. However, it should be noted that the predicted ensemble mean pressure head, $\langle\psi\rangle$, and concentration, $\langle C\rangle$ can be quite different from those observed in the field unless the ergodicity in terms of head and concentration is met.

3. Heterogeneous Vadose Zone and Numerical Setup

[7] To derive the effective unsaturated K and macrodispersivity, discussed in section 2, we considered a synthetic unsaturated zone. The unsaturated zone is a vertical, two-dimensional domain, 20 m wide and 20 m deep, and is discretized into 50 × 50 blocks with each block size being 0.4 m × 0.4 m. The medium within each block is considered as uniform, whose unsaturated hydraulic properties are assumed to follow *van Genuchten* [1980] and *Mualem* [1976] (vG-M) models:

$$\theta(\psi) = (\theta_s - \theta_r)[1 + (\alpha|\psi|)^n]^{-m} + \theta_r$$
$$K(\psi) = K_s\frac{\left(1 - (\alpha|\psi|)^{n-1}[1 + (\alpha|\psi|)^n]^{-m}\right)^2}{[1 + (\alpha|\psi|)^n]^{m/2}}, \tag{4}$$

where θ_s and θ_r are saturated and residual water contents, K_s is the saturated hydraulic conductivity, α and n are soil parameters, and $m = 1 - 1/n$.

[8] The media heterogeneity is represented by treating the vG-M parameters of each block as stochastic processes characterized by their means, standard deviations, and correlation functions. The means and standard deviations for each parameter are listed in Table 1 and are based on laboratory measurements of moisture retention and unsaturated K for coarse-textured sandy samples from the upper Hanford formation at the Hanford Site, Washington [*Khaleel*, 1999].

[9] Stochastic model results used to compare against the numerical results are based on the *Gardner* [1958] model,

$$K(\psi) = K_s\exp(\beta\psi), \tag{5}$$

where β is a fitting parameter. Equation (5) can be written as

$$\ln K(\psi) = \ln K_s + \beta\psi. \tag{6}$$

Equation (6) is referred to as the log linear model, since ln K is linearly related to ψ through the constant slope β. However, such a constant slope is often inadequate in describing ln $K(\psi)$ over ranges of tension of practical interest for field applications. As an alternative, the slope β can be approximated locally by straight lines over a fixed range of tension [*Polmann*, 1990]. The ln K_s term in equation (6) can then be derived by extrapolating the local slopes back to zero tension; the extrapolated K is denoted as K_0 to avoid confusion with K_s.

[10] To apply the Gardner model, unsaturated K values based on the vG-M model are divided into two ψ intervals (i.e., 0 to −1 m and −5 to −20 m). For each ψ interval the Gardner model is regressed against the conductivity data for each sample to obtain the parameter values for K_0 and β. The mean and standard deviation for the two parameters are listed in Table 2.

[11] A random field generator, based on Fast Fourier Transform [*Gutjahr*, 1989], is used to generate realizations for parameters K_s, α, and n and for each block in the flow domain. Parameters θ_r and θ_s are treated as deterministic constants because of their relatively

Table 2. Mean and Standard Deviation of Parameters for the Gardner Model

	Pressure Head −1.0 to 0.0 m		Pressure Head −20.0 to −5.0 m	
	Mean	Standard Deviation	Mean	Standard Deviation
ln K_0, m/d	0.253	0.771	−12.01	1.276
β, 1/m	8.133	1.493	0.37	0.040

small variability. A realization of the parameter fields is shown in Figure 1. The parameter fields are generated according to the spatial statistics specified in Table 1 and are considered independent of each other. However, any parameter field itself is correlated in space, characterized by an exponential correlation function. The integral scale of the exponential model for each parameter is assumed the same. The horizontal (λ_x) and vertical (λ_z) integral scales are 5 and 1 m, respectively. Each block is then divided into a number of elements (four elements in the vertical and one in the horizontal) to ensure accuracy of the numerical solution.

[12] To derive effective parameters in principal directions, two flow configurations are considered: (1) flow perpendicular to bedding (i.e., perpendicular to the direction of λ_x) and (2) flow parallel to bedding (i.e., parallel to the direction of λ_x). Note that flow parallel to bedding is analyzed by rotating the media for flow perpendicular to bedding (i.e., Figure 1) by 90°; the gradient remains parallel to gravity for both cases. A finite element code, MMOC2 [*Yeh et al.*, 1993], is used to solve equation (2) directly for steady state flow. No-flow boundaries are assigned to opposing sides of the flow domain. A method similar to that developed by *Harter and Yeh* [1993] is used to facilitate the convergence of the numerical solution for steady state infiltration in the presence of unit gradient. For a prescribed mean pressure head the infiltration rate is calculated based on mean values for ln K_s, α, and *n*. An initial guess of the ψ field is made in the presence of unit gradient condition in each block. A root-finding procedure is used to determine the ψ value corresponding to the calculated infiltration rate and the parameter values for each element. The calculated ψ values at the bottom boundary are then taken as the prescribed head boundary condition. The ψ values for the rest of the solution domain are then treated as our initial guesses for a prescribed flux at the top and a prescribed head boundary condition at the bottom.

[13] The flow simulations and the subsequent derivation of the effective unsaturated *K* are followed by transport simulations and the derivation of macrodispersivity. The MMOC2 is again used to simulate the concentration distribution of a conservative solute at various times for different mean pressure heads. The MMOC2 solves equation (3), using the modified method of characteristics.

[14] For the transport simulation, a zero initial concentration is assigned throughout the flow domain. A zero-concentration flux boundary is assigned to the left and right sides of the flow domain. A zero-diffusive flux boundary is assigned at the bottom. A prescribed concentration boundary that can vary with time but is uniform in space is used at the upper boundary to represent an instantaneous release of a conservative tracer. Both longitudinal and transverse local dispersivities at the mesh scale are assigned zero values so that the inherent numerical dispersion is the sole cause of local dispersion. The time step sizes used for each transport run under different mean pressure heads are chosen to avoid numerical instability and minimize numerical dispersion.

4. Methods of Analysis

[15] To derive the effective unsaturated hydraulic properties, four different approaches (i.e., analytical method, Monte Carlo simulations, direct averaging method, and tracer mass analysis), as described in sections 4.1, 4.2, 4.3, and 4.4, are used. A moment approach is used to obtain the macrodispersivity estimates.

4.1. Analytical Method

[16] The effective unsaturated *K* is determined using analytical expressions developed by *Yeh et al.* [1985a, 1985b] and *Yeh* [1989]. Assuming that the flow domain is perfectly stratified (i.e., $\lambda_x > \lambda_z$) and ln K_s and β are statistically independent, the

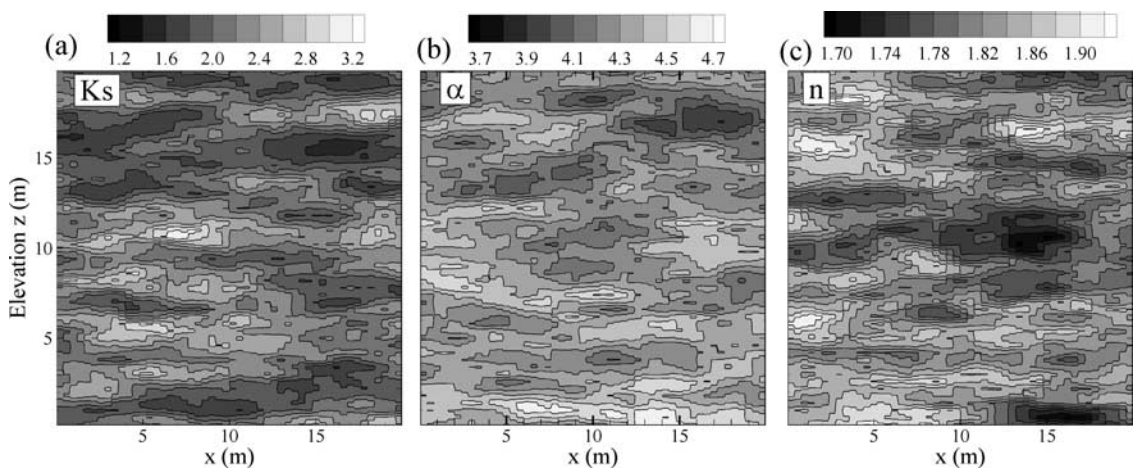

Figure 1. (a) K_s, (b) α, and (c) *n* parameter fields for a realization.

effective conductivity in two principal directions (i.e., flow perpendicular to bedding (K_V) and parallel to bedding (K_H)) are

$$K_V = \exp\left[F - \frac{\sigma_f^2}{2(1+B\lambda_z)} - \left(B - \frac{(2\lambda_z + |H|)}{2(1+B\lambda_z)}\sigma_\beta^2\right)|H|\right],$$
$$K_H = \exp\left[F + \frac{\sigma_f^2}{2(1+B\lambda_z)} - \left(B - \frac{(2\lambda_z - |H|)}{2(1+B\lambda_z)}\sigma_\beta^2\right)|H|\right], \quad (7)$$

where F is the mean of ln K_s, B is the mean of β, σ_f^2 is the variance of ln K_s, σ_β^2 is the variance of β, and H is the mean pressure head. The correlation functions for ln K_s and β are assumed to be exponential and have the same correlation length. Note that in applying equation (7) and in computing ln K_s statistics and correlation functions, ln K_s is replaced by ln K_0.

4.2. Monte Carlo Simulations

[17] The Monte Carlo (MC) simulations simulate steady state, gravity infiltration for 50 realizations of a heterogeneous medium. For a specified infiltration rate the simulated pressure head distributions for 50 realizations are averaged to yield a mean pressure head, H. Because the simulated flow field is under a unit mean gradient condition, the infiltration rate is equal to the effective conductivity at the calculated H. Repeating the procedure for different infiltration rates, we obtain the effective unsaturated K relationship. Similarly, we average the moisture content over the ensemble and the flow domain to derive an average θ that corresponds to the mean pressure head. Such averages of θ and H pairs constitute the effective moisture retention curve (MRC).

4.3. Direct Averaging Method

[18] The direct averaging method [*Yeh et al.*, 1985b] involves generating the conductivity value at a given pressure head for each element of the flow domain on the basis of the parameter values for a given realization. To derive the effective K for flow perpendicular to bedding and for flow parallel to bedding, the conductivity values for all elements over the number of realizations at a given ψ are averaged respectively using harmonic and arithmetic averaging, as in saturated media. A similar approach is also used to derive the effective MRC. In this case, an arithmetic averaging of the θ values (generated on the basis of the model and parameter values for a given ψ) for all elements of the flow domain and realizations is used to obtain an average θ at a given ψ. Note that direct averaging is also a particular case of the anisotropic power averaging scheme [*Ababou et al.*, 1991].

4.4. Tracer Mass Analysis

[19] In this analysis, a moment method, described later (section 4.5), is used to determine the position of the center of the simulated ensemble-mean tracer plume at various times. The velocity of the center of the plume is then determined. The product of the velocity and the average water content approximates the mean infiltration flux, which is equivalent to the effective K at the mean pressure head when the flow is under a unit mean gradient condition ($\langle J \rangle = 1$), i.e.,

$$\langle q \rangle = K^e \langle J \rangle = K^e. \quad (8)$$

The procedure is applied to flow perpendicular and parallel to bedding to obtain the effective conductivity along both principal directions.

4.5. Moment Analysis for Macrodispersivity

[20] For a given steady flow and a prescribed flux the migration and spread of a slug of tracer is simulated. Snapshots are taken of the two-dimensional plume distribution at different times. The snapshot at each sampling time is then averaged over the length across the flow domain to obtain the solute concentration profiles as a function of depth. The concentration profiles for all realizations are averaged to obtain the ensemble mean profile. These profiles are then used to evaluate their spatial moments using

$$M(i) = \int z^i \theta^i(z) C^i(z,t) dz, \quad (9)$$

where $M(i)$ is the ith moment of the solute plume, and the superscript, i, refers to the ith order of the moment. The zero moment, $M(0)$, is the total mass for a concentration profile; $M(1)$ corresponds to the location of the center of mass at time t; $M(2)$ represents the spread of the plume around its center; and $M(3)$ describes the skewness of the plume profile.

[21] The calculated second spatial moment of the plume about the center of mass (i.e., spatial variance) over time allows estimation of the longitudinal macrodispersivity [*Harter and Yeh*, 1996]. Specifically, for both principal directions the time derivative of the intermediate stage of the spatial variance, where the variance is approximately linearly proportional to time, yields the longitudinal macrodispersion coefficient, D, i.e.,

$$\frac{1}{2}\frac{\partial \sigma^2}{\partial t} = D, \quad (10)$$

where σ^2 is the spatial variance and t is time. Again, the moment data for early and late times are ignored to avoid possible boundary effects. The macrodispersivity, A, is defined as

$$A = D/\langle V \rangle. \quad (11)$$

5. Results and Discussion

5.1. Simulated Flow Fields and Trajectories for a Single Realization

[22] For the parameter fields shown in Figure 1, the simulated pressure head field and flow trajectories for flow perpendicular to bedding and for mean pressure heads, H, of -1, -5, -10, and -20 m are illustrated in Figure 2. Results for flow parallel to bedding are shown in Figure 3.

[23] As shown in Figures 2 and 3, the head pattern changes as the medium moves from a less negative H to a more negative H value. For $H = -1$ m, the head variation is negligible, and for the particular boundary conditions considered, the flow field tends to be one-dimensional (vertical downward), regardless of flow being perpendicular (Figure 2a) or parallel to bedding (Figure 3a). As H becomes more negative, the head variation becomes more noticeable. The variation is the greatest at $H = -20$ m. These results agree with the finding that the head variability increases as the mean pressure head becomes more negative or the medium becomes less saturated [*Yeh et al.*, 1985a, 1985b]. Similar results were also reported by other investigators [e.g., *Wildenschild and Jensen*, 1999b; *Harter and Yeh*, 1996]. Our results, of course, are based on uncorrelated α and ln K_s. With a positive correlation of α and ln K_s, the variability can approach zero and then increase [*Yeh*, 1989; *Ababou*, 1988].

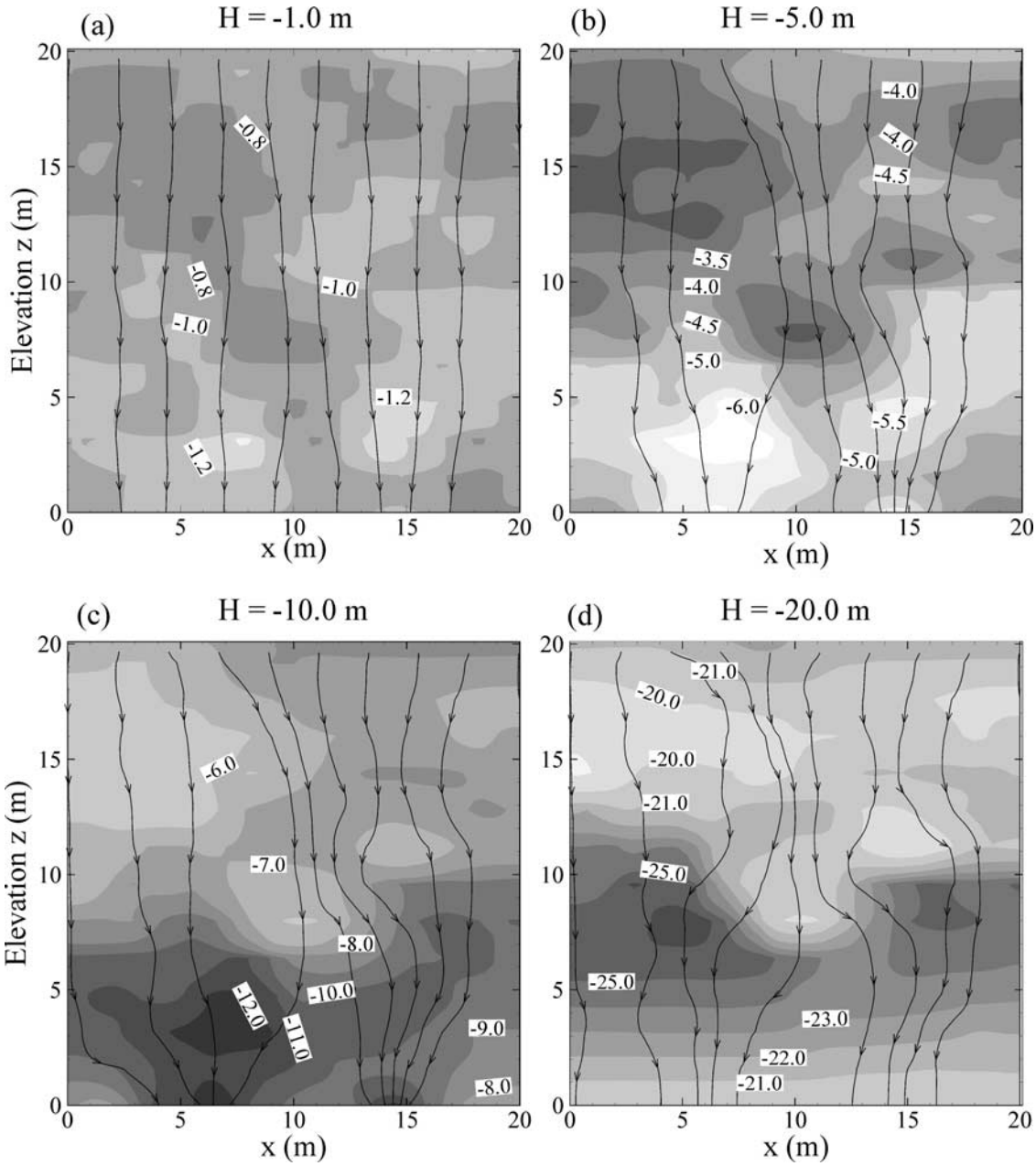

Figure 2. Simulated pressure head field and streamlines for flow perpendicular to bedding for mean pressure heads, H, of (a) −1 m, (b) −5 m, (c) −10 m, and (d) −20 m.

[24] Also, the trajectories are nearly straight and vertical at low mean tensions (Figures 2a and 3a) and become more tortuous at mean tensions in excess of 1 m (Figures 2b–2d and Figures 3b–3d). *Wildenschild and Jensen* [1999b] and *Harter and Yeh* [1996] also observed an increase in tortuosity with a decrease in saturation. It is interesting to note that the tortuosity of the flow path appears to be less for flow parallel to bedding (Figure 3) than for flow perpendicular to bedding (Figure 2). As discussed later (section 5.3), this finding sheds light on the effect of bedding orientation on macrodispersion. Our results for the pressure heads and the associated trajectories in Figures 2 and 3 also are similar to those of *Ursino et al.* [2000], who studied upscaling of unsaturated conductivity for different pore-scale geometries for mean tensions of up to 1.6 m. Similar to our findings, Ursino et al. also observed less tortuosity in their ''column'' system (analogous to parallel to bedding) than in their ''layer'' system (analogous to perpendicular to bedding).

5.2. Effective Unsaturated Hydraulic Properties

[25] Effective unsaturated K curves based on the MC simulation, analytical, direct averaging, and tracer analyses are shown in Figures 4a and 4b for flow perpendicular and parallel to bedding, respectively. In general, the numerical results compare favorably to results based on the analytical solution and suggest dependence of macroscopic hydraulic anisotropy on the mean pressure head (Figure 5). This is an important result, considering the fact that the stochastic theory, although widely used and cited, has not been tested otherwise for the relatively high-tension regime considered in this work. Unlike our work, other studies [e.g., *McCord et al.*,

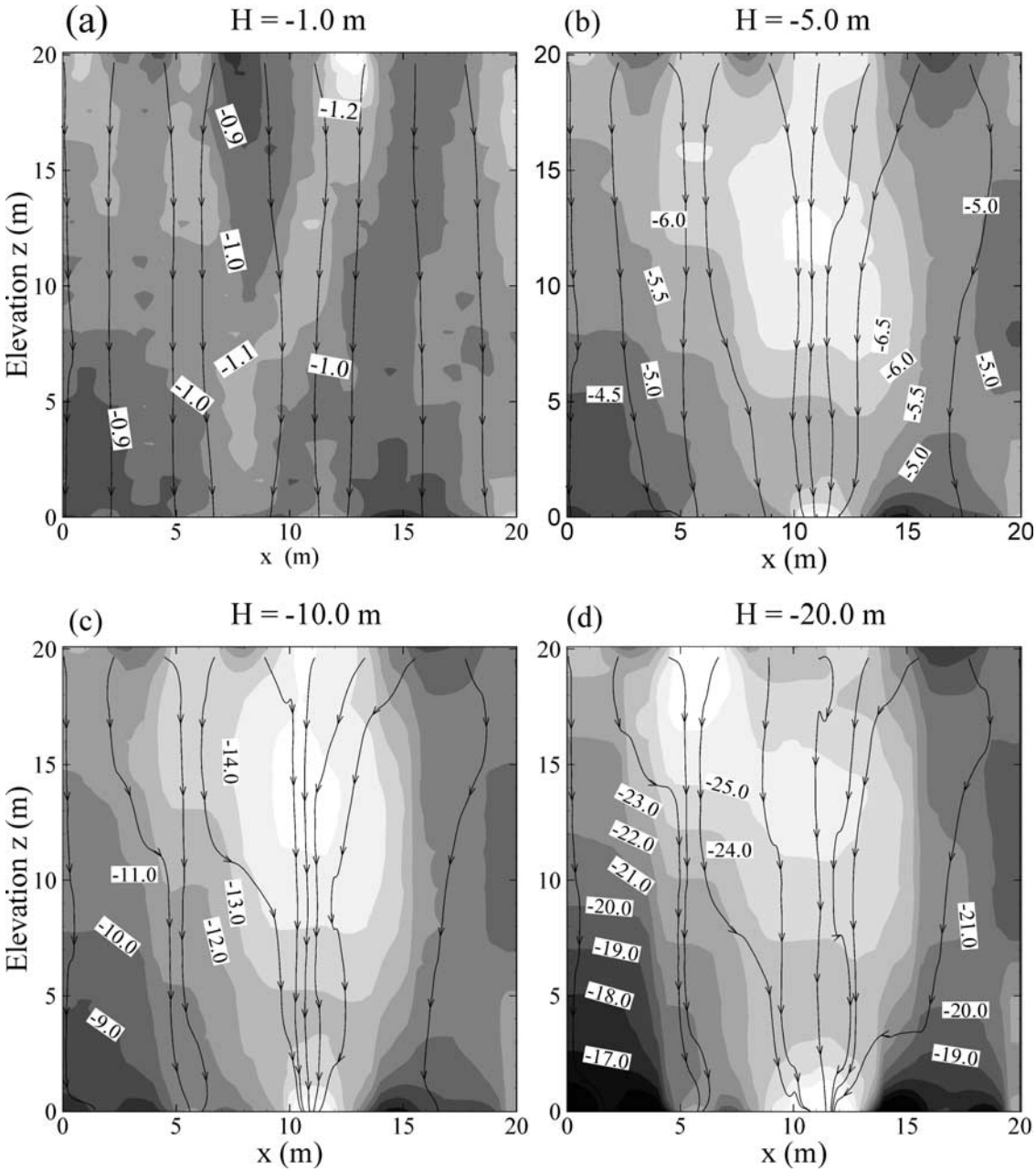

Figure 3. Simulated pressure head field and streamlines for flow parallel to bedding for mean pressure heads, H, of (a) -1 m, (b) -5 m, (c) -10 m, and (d) -20 m (note that flow parallel to bedding is analyzed by rotating the media used for flow perpendicular to bedding by 90°).

1991; *Yeh and Harvey*, 1990; *Wildenschild and Jensen*, 1999a, 1999b] are for a much lower-tension regime.

[26] As with the analytical method (equation (7)), the direct averaging also produces the tension-dependent, anisotropic, unsaturated effective K (Figures 4 and 5). However, for the tension range of interest, direct averaging yields a consistently higher anisotropy than the stochastic method. For direct averaging, the arithmetically averaged values yield the upper bound for the effective unsaturated K, as in saturated flow, whereas the harmonically averaged values yield the lower bound. The large differences (Figures 4 and 5) are attributed to the fact that, as in saturated flow, the direct averaging assumes a constant pressure head gradient over each homogeneous soil block. In reality, the gradient varies with ψ because of the dependence of K on ψ. In other words, direct averaging does not consider the actual flow behavior and thus exaggerates the variability of conductivity between blocks and yields unrealistic values for the effective K [*Yeh et al.*, 1985b].

[27] It is interesting to note that the effective K values derived from the MC simulation for both flow regimes are reasonably close to those based on the velocity of the center of the tracer mass (Figures 4a and 4b). This implies that the estimated conductivity curves using the MC simulation correctly predict the movement of the center of the solute plume. Therefore they do indeed represent the effective unsaturated K for the flow field.

[28] Note that the analytical method was applied to derive the effective K over the ψ range (-5 to -20 m) from which the spatial statistics of the Gardner model were derived. As shown in Figure 4b, the effective K in the direction parallel to bedding,

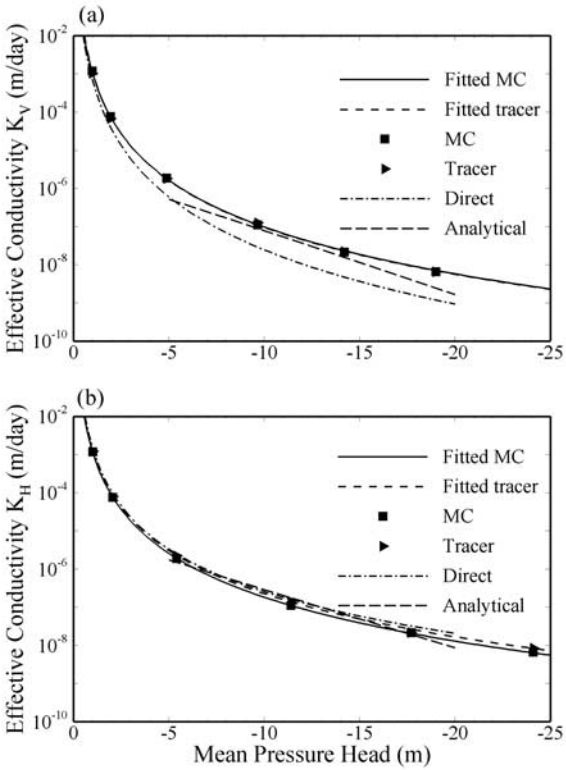

Figure 4. Effective hydraulic conductivity for flow (a) perpendicular to bedding and (b) parallel to bedding (both Monte Carlo (MC) and direct data are flow-based averages, whereas tracer data are tracer-based K; the fitted MC and tracer data overlay each other in Figure 4a).

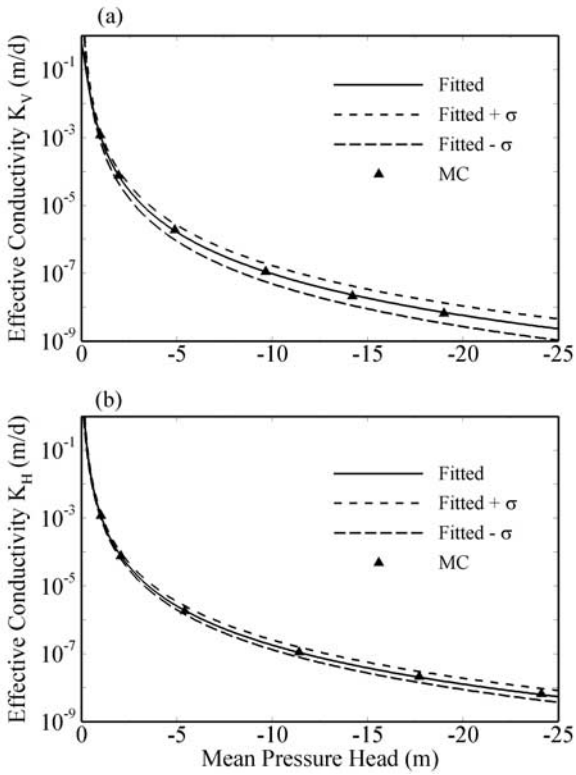

Figure 6. Standard deviation for the effective hydraulic conductivity for flow (a) perpendicular to bedding and (b) parallel to bedding.

based on the analytical solution, is close to both the numerical and tracer data. However, the conductivity in the direction perpendicular to bedding, based on the analytical solution, is somewhat different from both numerical and tracer data (Figure 4a). This difference may be due to the fact that the unsaturated K for the MC simulations are based on the vG-M model, whereas those for the analytical solution are based on the Gardner model. Consequently, the spatial statistics based on the Gardner model are not expected to reproduce the spatial variability characterized by the vG-M model over a broad range of ψ (i.e., -5 to -20 m). In order to obtain a better agreement, the unsaturated K data should be divided over a range of smaller ψ intervals in which the two models produce near identical K. That is, the spatial statistics of parameters for the Gardner model should be treated as a function of ψ.

[29] The effective properties from the stochastic theory are ensemble-average properties, which can be quite different from the spatially averaged properties that involve only a single realization of the heterogeneity. The ensemble properties will be equivalent to the spatially averaged properties if the spatial scale of the flow domain is large compared with the correlation scale of the

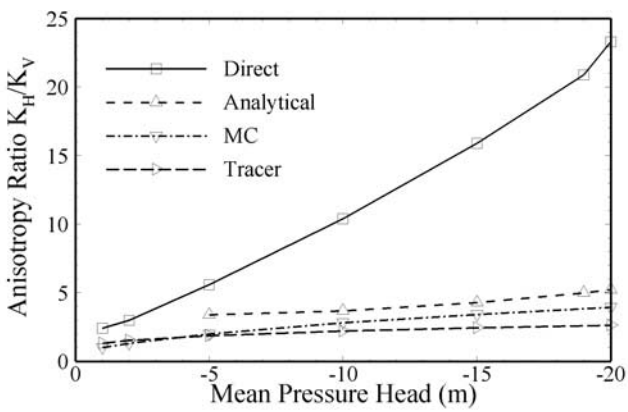

Figure 5. Macroscopic anisotropy (ratio of K parallel to bedding to K perpendicular to bedding) based on four different methods.

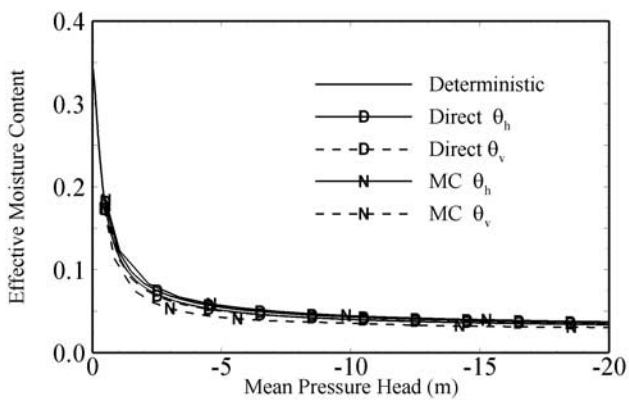

Figure 7. Effective moisture retention curves based on different methods (θ_h and θ_v refer to averaging for flow parallel to bedding and perpendicular to bedding, respectively; both MC and direct data are flow-based averages).

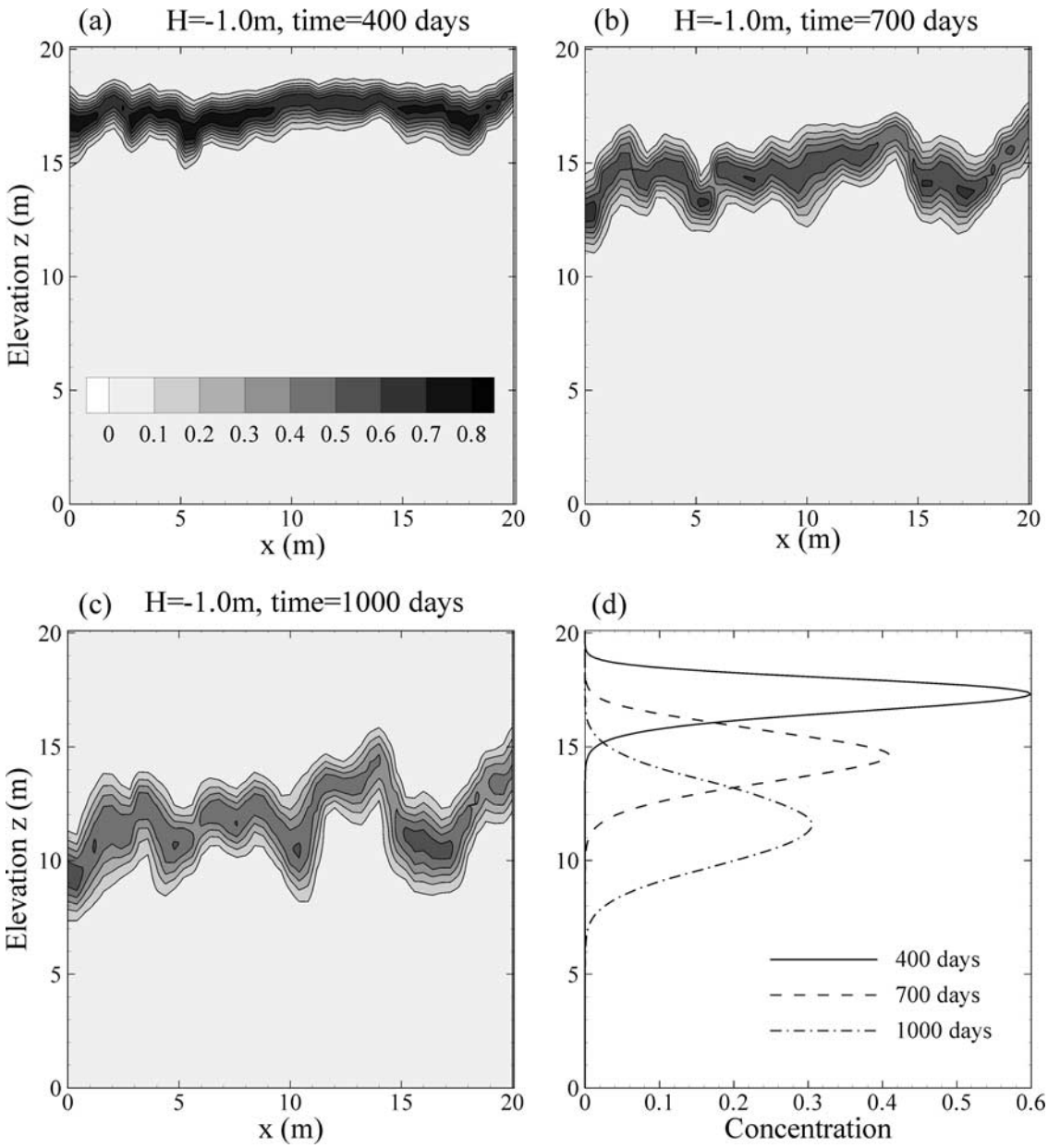

Figure 8. Simulated concentration distribution for a single realization at (a) 400 days, (b) 700 days, and (c) 1000 days and (d) the averaged concentration profile at those times for flow perpendicular to bedding for a mean pressure head of −1 m.

heterogeneous flow field. Deviation of the spatially averaged effective K of individual realizations from the ensemble average for the two flow regimes is indicated in Figure 6 by the standard deviation (SD). However, the SD is smaller for flow parallel to bedding than for perpendicular to bedding. More importantly, the SD data indicate that the lower bound of the effective K for flow parallel to bedding is as large as the upper bound of the effective K for flow perpendicular to bedding. This suggests that the moisture-dependent anisotropy exists not only in the ensemble property but also in the individual realizations.

[30] The effective MRCs (Figure 7) derived from the MC simulations show some but small anisotropy (they almost overlay each other). However, this property, in theory, must be scalar. This anisotropy may be a consequence of the small domain size used in the simulation. Nonetheless, the curves are very close to the MRC estimated on the basis of a deterministic approach that uses an arithmetic average of all the θ values generated for each element at a given ψ using the parameters specified for that element.

5.3. Analysis of Concentration Distribution and Macrodispersivity

[31] For both cases of flow perpendicular and parallel to bedding, snapshots were taken at several times of the simulated two-dimensional plume. At each sampling time, the two-dimensional plume was averaged over the length across the flow domain to obtain the concentration profiles as a function of distance along the flow direction. A space/ensemble averaging was used, with spatial averaging being performed only along directions of statistical homogeneity. Fifty averaged profiles corresponding to the 50 random fields were averaged to obtain the ensemble concentration profile. As discussed later, the ensemble profiles were then used to evaluate their spatial moments using equation (10).

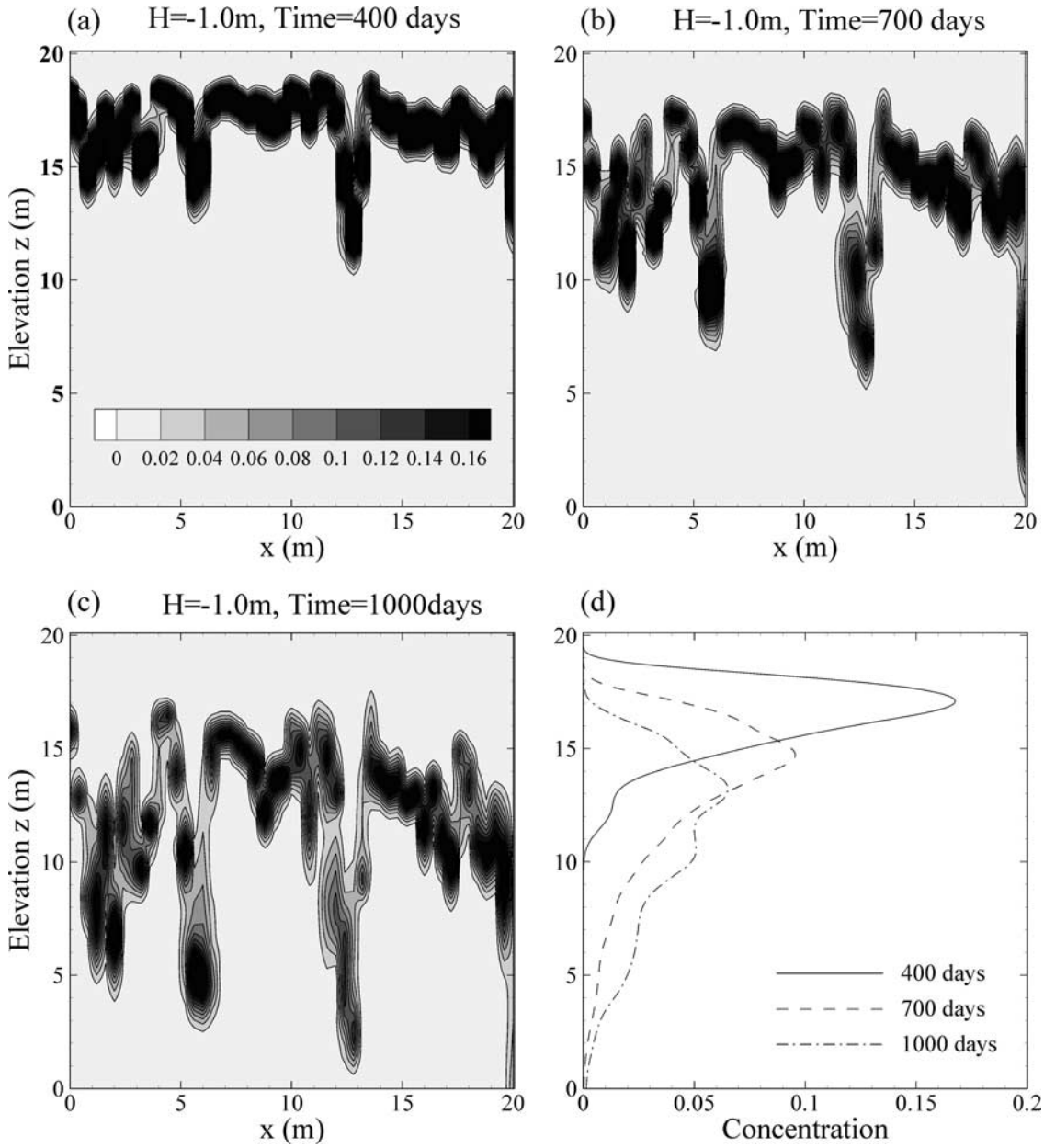

Figure 9. Simulated concentration distribution for a single realization at (a) 400 days, (b) 700 days, and (c) 1000 days and (d) the averaged concentration profile at those times for flow parallel to bedding for a mean pressure head of −1 m (note that flow parallel to bedding is analyzed by rotating the media used for flow perpendicular to bedding by 90°).

[32] Figures 8a, 8b and 8c are snapshots of the simulated plume for a single realization and for flow perpendicular to bedding at 400, 700, and 1000 days after release of a conservative tracer across the top boundary of the heterogeneous media (Figure 1). Similarly, Figures 9a, 9b, and 9c are snapshots of the plume at identical sampling times for flow parallel to bedding for the same single realization (Figure 1).

[33] Both flow regimes (Figures 8 and 9) are for a mean pressure head of −1.0 m. The averaged concentration profiles for the two flow regimes and for the corresponding sampling times are illustrated in Figures 8d and 9d. A comparison of Figures 8 and 9 shows that the two-dimensional concentration distribution is more erratic in the case of flow parallel to bedding than for flow perpendicular to bedding (Figures 9a, 9b, and 9c versus Figures 8a, 8b, and 8c). Bedding perpendicular to flow direction enhances lateral mixing and prevents rapid growth of preferential flow paths. On the contrary, bedding parallel to flow facilitates preferential flow, leaving solute trapped in low permeable regions behind. Small numerical dispersion is the only lateral mixing mechanism. Consequently, the averaged concentration profiles for flow perpendicular to bedding (Figure 8d) exhibit the typical bell-shaped distribution as described by the Fickian convection-dispersion equation. On the contrary, the concentration profiles for flow parallel to bedding are highly skewed and characterized by multiple peaks, and spread out over greater distances, characteristics of a non-Fickian behavior. In addition, Figure 9 suggests an enhanced tailing and increasingly preferential flow with the distance traveled. Similar results were also reported by *Wildenschild and Jensen* [1999b]. This suggests that a dead-end pore model [*Coats and Smith*, 1964] or a mobile-immobile (MIM) zone model [e.g., *Bond and Wierenga*,

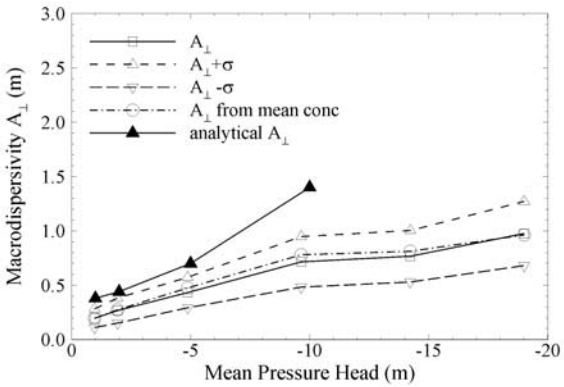

Figure 10. Longitudinal macrodispersivity as a function of mean pressure head for flow perpendicular to bedding.

1990] may be an appropriate model for reproducing solute profiles similar to those in Figure 9. Nonetheless, on the basis of results of soil column experiments, *Padilla et al.* [1999] speculated that the fitted parameters of the MIM model might vary with the length of the experiment until the Fickian regime is fully established. Results of our study lead us to further speculate that the parameter values for a MIM transport model will depend on the relationship between the flow direction and the longitudinal axis of the heterogeneity.

[34] Notice that Figures 8 and 9 depict the actual two-dimensional concentration distribution for a single realization of the heterogeneous media. These actual concentration distributions can be quite different from the ensemble-mean concentrations, based on the convection-dispersion equation (3) or a MIM model using effective properties. While the two-dimensional mean concentrations are not shown, their distribution over the length across the flow domain will be similar to the average concentration profiles shown in Figures 8d and 9d, provided the ergodicity is met. Hence it is apparent that the disagreement between the actual and the ensemble mean concentrations is far greater for flow parallel to bedding than for flow perpendicular to bedding. In other words, the concentration variance (or uncertainty) associated with the mean concentration predicted by the effective K and macrodispersion approach is greater for flow parallel to bedding than for flow perpendicular to bedding.

[35] Plots (not shown here) of the second and third moments as a function of time for different mean pressure head fields also support the preceding observations. For flow perpendicular to bedding the second moment was found to increase at some constant rate after a short period. The third moment (i.e., skewness) of the plume was generally very small, indicating Gaussian concentration distributions. On the contrary, values of the third moment for flow parallel to the bedding were large, indicating non-Gaussian concentration distribution (i.e., non-Fickian behavior). These results suggest that the Fickian regime is reached much earlier for cases with flow perpendicular to bedding than for those with flow parallel to bedding. Furthermore, it was found that the skewness increased with an increase in mean tension of the flow field. *Padilla et al.* [1999] observed a similar behavior in soil column experiments as the soil was desaturated.

[36] Figures 10 and 11 illustrate the asymptotic longitudinal macrodispersivity estimates for flow perpendicular and parallel, respectively, to bedding. For both cases, dispersivity increases with an increase in mean tension. However, the longitudinal macrodispersivity for flow parallel to bedding is much greater than for flow perpendicular to bedding.

5.4. Comparison of Macrodispersivities with Stochastic Estimates

[37] As a check on the trend in dispersivity estimates for flow parallel and perpendicular to bedding, an attempt was made to compare the numerical estimates with those based on stochastic theory. With the flow being steady and under gravity drainage (unit-mean gradient), existing stochastic results for saturated media are adopted for unsaturated media. The variance of unsaturated K is the primary controlling factor for macrodispersivity. Therefore, for application to unsaturated media, the variance of ln K_s is replaced with the variance of log unsaturated K. To obtain stochastic estimates, each flow configuration was treated separately.

[38] *Mantoglou and Gelhar* [1985] derived approximate expressions for macrodispersivities in unsaturated media for flow perpendicular to bedding. They showed that the asymptotic value of tension-dependent longitudinal macrodispersivity, $A_\perp$, under unit mean gradient condition, is

$$A_\perp(H) = \frac{\sigma^2_{\mathrm{LnK}}\lambda_z}{\gamma^2}, \tag{12}$$

where $A_\perp$ depends on the mean pressure head H, σ^2_{LnK} is the variance in log unsaturated K, and γ is a flow factor that depends on the direction of mean flow and the orientation of heterogeneity. Equation (12) represents the asymptotic macrodispersivity estimate for steady state uniform flow with uniform mean tension. Again, it applies to a plume that is much larger than the size of the heterogeneity and has been displaced for a large distance. Note that σ^2_{LnK} in equation (12) becomes rather large for dry soils. In our case, at a tension of 1 m, σ^2_{LnK} is about one, whereas at a tension of 20 m, σ^2_{LnK} is about three.

[39] To apply equation (12), an estimate of λ_z for unsaturated K is needed. As discussed earlier, a λ_z of the order of 1 m was used for the MC simulations. However, as the saturation decreases, an increase in the variance of log conductivity is expected to be compensated in part by a decrease in the correlation scale of log unsaturated K [*Russo*, 1993]. Also, the γ factor in a predominantly vertical unsaturated flow through a layered system would be less than 1; it is approximately the ratio of the harmonic and geometric means of unsaturated K. Using a correlation length of 10 cm (approximate measurement scale for small-scale measurements for unsaturated K), and γ estimates based on the ratio of the harmonic

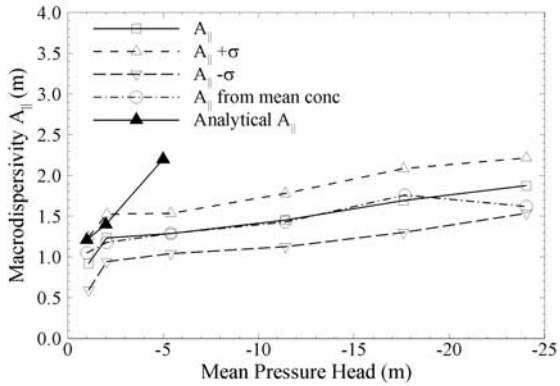

Figure 11. Longitudinal macrodispersivity as a function of mean pressure head for flow parallel to bedding (note that flow parallel to bedding is analyzed by rotating the media used for flow perpendicular to bedding by 90°).

and geometric means, we obtained dispersivity estimates perpendicular to bedding that are on the order of tens of centimeters at relatively low tensions of up to 2 m (Figure 10). These estimates are of the same order of magnitude as those based on ensemble-averaged MC simulations. The stochastic-based solutions quickly diverge from the ensemble averages at higher mean tensions that are on the order of tens of meters, suggesting that a direct application of equation (12) to relatively dry soils is inappropriate. Nonetheless, it is encouraging to note that in spite of simplifying assumptions, the numerical estimates compare favorably, at low tensions, with those based on equation (12).

[40] For flow parallel to bedding, we again estimated macrodispersivities through a relatively simple extension of the saturated media theory. For stratified media with flow parallel to bedding, *Gelhar and Axness* [1983] derived an equation for longitudinal macrodispersivity, $A_{||}$:

$$A_{||}(H) = \frac{1.31\lambda_x^{0.5}\sigma_{\mathrm{LnK}}^2\lambda_z}{\gamma^2\alpha_T^{0.5}}. \qquad (13)$$

A λ_x of 5 m was used for the MC simulations. However, similar to λ_z, with a decrease in saturation, we expect a decrease in the correlation scale of log unsaturated K. Using $\lambda_x = 30$ cm ($\lambda_x > \lambda_z$), and a local transverse dispersivity, α_T, of 5 cm, we obtain, at low tensions of up to 2 m, macrodispersivity estimates of the order of 1 m for flow parallel to bedding. Again, these are of the same order of magnitude as those based on the Monte Carlo ensemble average (Figure 11). However, at higher tensions, we notice considerable disagreement between the ensemble averages and the stochastic results. Apparently, with an increase in σ_{LnK}^2, there is a greater deviation between the numerical and stochastic solutions. The lack of a reasonable agreement between the numerical and stochastic solutions at high tensions raises questions regarding *Russo*'s [1993] conclusion about vadose zone macrodispersivities being defined in a manner similar to those for saturated media.

6. Summary and Concluding Remarks

[41] Ensemble-averaged effective unsaturated conductivities are derived on the basis of MC simulation, stochastic/analytical, direct averaging, and tracer mass methods for two principal directions (flow perpendicular and flow parallel to bedding). Results show that macroscopic anisotropy of the effective unsaturated K increases with increasing tension, but the increase is rather mild for the heterogeneous media considered in this work. Estimates based on stochastic formulas compare well with the ensemble average of MC estimates for effective unsaturated K. This is an important result, considering the fact that the stochastic theory, although widely used and cited, has not been tested otherwise for the relatively high-tension regime considered in this work, where the first-order approximation may fail.

[42] Longitudinal macrodispersivity depends on the mean pressure head; it increases as the soil becomes drier. Longitudinal macrodispersivity values for flow parallel to bedding are greater than those for flow perpendicular to bedding. While the averaged concentration profiles for flow perpendicular to bedding show approximate Fickian behavior, the averaged profiles for flow parallel to bedding are highly skewed and non-Fickian. Comparisons of the actual two-dimensional concentration distributions and the average concentration profiles suggest that the ensemble mean concentration can be very different from the actual concentration distribution for flow parallel to bedding.

[43] For both flow regimes of parallel and perpendicular to bedding, the macrodispersivities based on stochastic theory compare reasonably well to the numerical ensemble averages for mean tensions of the order of 100 cm. However, with an increase in variance of log unsaturated K, we notice an increase in deviation between the numerical and stochastic solutions. The lack of a reasonable agreement between the numerical and stochastic solutions at high tensions raises questions about vadose zone macrodispersivities being defined in a manner similar to those for saturated media.

[44] **Acknowledgments.** The support provided by Fred Mann (CH2M Hill Hanford Group, Inc.) and the Hanford Immobilized Low-Activity Tank Waste Program is gratefully acknowledged. Suggestions provided by the Associate Editor and two anonymous reviewers are greatly appreciated. The work reported was performed for the U.S. Department of Energy under Contract DE-AC06-99RL14047. Reference herein to any specific commercial product, process, or service by trade name, trademark, manufacturer, or otherwise, does not necessarily constitute or imply its endorsement, recommendation, or favoring by the United States Government or any agency thereof or its contractors or subcontractors. The views and opinions of the authors do not necessarily state or reflect those of the United States Government or any agency thereof.

References

Ababou, R., Three-dimensional flow in random porous media, Ph.D. thesis, Mass. Inst. of Technol., Cambridge, Mass., 1988.

Ababou, R., A. C. Bagtzoglou, B. Sagar, and G. Wittmeyer, Stochastic analysis of flow and transport, in *Report on Research Activities for Calendar Year 1990*, *Rep. NUREG/CR-5817*, edited by W. C. Patrick, Chap. 6, U.S. Nucl. Regul. Comm., Washington, D. C., 1991.

Bagtzoglou, A. C., S. Mohanty, A. Nedungadi, T.-C. J. Yeh, and R. Ababou, Effective hydraulic property calculations for unsaturated fractured rock with semi-analytical and direct numerical techniques: Review and applications, *Rep. 94-007*, Cent. for Nucl. Waste Regul. Anal., Southwest Res. Inst., San Antonio, Tex., 1994.

Birkholzer, J., and C.-F. Tsang, Solute channeling in unsaturated heterogeneous media, *Water Resour. Res.*, *33*, 2221–2238, 1997.

Bond, W. J., and P. J. Wierenga, Immobile water during solute transport in unsaturated sand columns, *Water Resour. Res.*, *26*, 2475–2481, 1990.

Coats, K. H., and B. D. Smith, Dead end pore volume and dispersion in porous media, *Soc. Pet. Eng. J.*, *4*, 73–84, 1964.

Desbarats, A. J., Scaling of constitutive relationships in unsaturated heterogeneous media, *Water Resour. Res.*, *34*, 1427–1436, 1998.

Gardner, W. R., Some steady-state solutions of the unsaturated moisture flow equation with applications to evaporation from a water table, *Soil Sci.*, *85*, 228–232, 1958.

Gelhar, L. W., *Stochastic Subsurface Hydrology*, 390 pp., Prentice-Hall, Englewood Cliffs, N. J., 1993.

Gelhar, L. W., and C. L. Axness, Three-dimensional analysis of macrodispersion in a stratified aquifer, *Water Resour. Res.*, *19*, 161–180, 1983.

Green, T. R., and D. L. Freyberg, State-dependent anisotropy: Comparisons of quasi-analytical solutions with stochastic results for steady gravity drainage, *Water Resour. Res.*, *31*, 2201–2212, 1995.

Gutjahr, A. L., Fast Fourier transforms for random field generation, project report, 106 pp., N. M. Tech, Socorro, N. M., 1989.

Harter, T., and T.-C. J. Yeh, An efficient method for simulating steady unsaturated flow in random porous media: Using an analytical perturbation solution as initial guess to a numerical model, *Water Resour. Res.*, *29*, 4139–4149, 1993.

Harter, T., and T.-C. J. Yeh, Stochastic analysis of solute transport in heterogeneous, variably saturated soils, *Water Resour. Res.*, *32*, 1585–1596, 1996.

Khaleel, R., *Far-Field Hydrology Data Package for Immobilized Low-Activity Tank Waste Performance Assessment*, *HNF-4769*, revision 1, Fluor Daniel Northwest, Richland, Wash., 1999.

Mantoglou, A., and L. W. Gelhar, Large scale models of transient unsaturated flow and contaminant transport using stochastic methods, *Tech. Rep. 299*, Ralph M. Parsons Laboratory, Mass. Inst. of Technol., Cambridge, Mass., 1985.

Mantoglou, A., and L. W. Gelhar, Stochastic modeling of large-scale transient unsaturated flow, *Water Resour. Res.*, *23*, 37–46, 1987.

McCord, J. T., D. B. Stephens, and J. L. Wilson, Hysteresis and state-dependent anisotropy in modelling unsaturated hillslope hydrologic processes, *Water Resour. Res.*, *27*, 1501–1518, 1991.

Mualem, Y., A new model for predicting the hydraulic conductivity of unsaturated porous media, *Water Resour. Res.*, *12*, 513–522, 1976.

Mualem, Y., Anisotropy of unsaturated soils, *Soil Sci. Soc. Am. J.*, *48*, 505–509, 1984.

Padilla, I. Y., T.-C. J. Yeh, and M. H. Conklin, The effect of water content on solute transport in unsaturated porous media, *Water Resour. Res.*, *35*, 3303–3313, 1999.

Polmann, D. J., Application of stochastic methods to transient flow and transport in heterogeneous unsaturated soils, Ph.D. thesis, Mass. Inst. Technol., Cambridge, Mass., 1990.

Polmann, D. J., D. McLaughlin, S. Luis, L. W. Gelhar, and R. Ababou, Stochastic modeling of large-scale flow in heterogeneous unsaturated soils, *Water Resour. Res.*, *27*, 1447–1458, 1991.

Roth, K., and K. Hammel, Transport of conservative chemical through an unsaturated two-dimensional Miller-similar medium with steady state flow, *Water Resour. Res.*, *32*, 1653–1663, 1996.

Russo, D., Stochastic modeling of macrodispersion for solute transport in a heterogeneous unsaturated porous formation, *Water Resour. Res.*, *29*, 383–397, 1993.

Stephens, D. B., and S. Heermann, Dependence of anisotropy on saturation in a stratified sand, *Water Resour. Res.*, *24*, 770–778, 1988.

Ursino, N., K. Roth, T. Gimmi, and H. Flühler, Upscaling of anisotropy in unsaturated Miller-similar porous media, *Water Resour. Res.*, *36*, 421–430, 2000.

van Genuchten, M. T., A closed-form solution for predicting the conductivity of unsaturated soils, *Soil Sci. Soc. Am. J.*, *44*, 892–898, 1980.

Wildenschild, D., and K. H. Jensen, Laboratory investigations of effective flow behavior in unsaturated heterogeneous sands, *Water Resour. Res.*, *35*, 17–27, 1999a.

Wildenschild, D., and K. H. Jensen, Numerical modeling of observed effective flow behavior in unsaturated heterogeneous sands, *Water Resour. Res.*, *35*, 29–42, 1999b.

Yeh, T.-C. J., One-dimensional steady-state infiltration in heterogeneous soils, *Water Resour. Res.*, *25*, 2149–2158, 1989.

Yeh, T.-C. J., Scale issues of heterogeneity in vadose zone hydrology, in *Scale Dependence and Scale Invariance*, edited by G. Sposito, Cambridge Univ. Press, New York, 1998.

Yeh, T.-C. J., and D. J. Harvey, Effective unsaturated hydraulic conductivity of layered sands, *Water Resour. Res.*, *26*, 1271–1279, 1990.

Yeh, T.-C. J., L. W. Gelhar, and A. L. Gutjahr, Stochastic analysis of unsaturated flow in heterogeneous soils, 1, Statistically isotropic media, *Water Resour. Res.*, *21*, 447–456, 1985a.

Yeh, T.-C. J., L. W. Gelhar, and A. L. Gutjahr, Stochastic analysis of unsaturated flow in heterogeneous soils, 2, Statistically anisotropic media with variable α, *Water Resour. Res.*, *21*, 457–464, 1985b.

Yeh, T.-C. J., R. Srivastava, A. Guzman, and T. Harter, A numerical model for two dimensional flow and chffmical transport, *Groundwater*, *31*, 634–644, 1993.

R. Khaleel, Fluor Federal Services, P.O. Box 1050, Richland, WA 99352, USA. (raziuddin_khaleel@rl.gov)

Z. Lu, Earth and Environmental Science Division, Los Alamos National Laboratory, Los Alamos, NM 87545, USA. (zhiming@vega.lanl.gov)

T.-C. J. Yeh, Department of Hydrology and Water Resources, University of Arizona, Tucson, AZ 85721, USA. (ybiem@mac.hwr.arizona.edu)